

# Spectroscopic and Mechanistic Studies of Type-1 and Type-2 Copper Sites in *Pseudomonas aeruginosa* Azurin As Obtained by Addition of External Ligands to Mutant His46Gly<sup>†</sup>

Gertie van Pouderoyen,<sup>‡</sup> Colin R. Andrew,<sup>§</sup> Thomas M. Loehr,<sup>§</sup> Joann Sanders-Loehr,<sup>§</sup> Shyamalava Mazumdar,<sup>||</sup> H. Allen O. Hill,<sup>||</sup> and Gerard W. Canters<sup>\*,‡</sup>

Leiden Institute of Chemistry, Gorlaeus Laboratories, Leiden University, 2300 RA Leiden, The Netherlands, Department of Chemistry, Biochemistry and Molecular Biology, Oregon Graduate Institute of Science and Technology, Portland, Oregon 97291-1000, and Inorganic Chemistry Laboratory, University of Oxford, Oxford, U.K.

Received July 14, 1995; Revised Manuscript Received November 17, 1995<sup>®</sup>

**ABSTRACT:** The spectroscopic and mechanistic properties of the Cu-containing active site of azurin from *Pseudomonas aeruginosa* were investigated by the construction of a mutant in which one of the ligands of the metal, His46, was replaced by a glycine. Although the mutation creates a hole in the interior of the protein, the 3D structure of the protein does not change to any appreciable extent. However, the spectroscopic (optical, resonance Raman, EPR) properties of the mutant protein are strongly affected by the mutation. In the presence of external ligands, the properties of the original wild-type protein are restored to a smaller or larger extent, depending on the ligand. It is concluded that the hole created by the mutation, even though it is completely buried inside the protein, can be filled by external ligands, often resulting in the creation of a mixture of so-called type-1 and type-2 copper sites. Also, the redox properties (midpoint potential, kinetics of reduction/oxidation) appeared to be strongly affected by the mutation and the presence of external ligands. The results are compared with previous results obtained on the mutant His117Gly.

The unique spectroscopic properties of mononuclear blue copper (type-1) proteins have made them the object of many experimental and theoretical studies. Oxidized type-1 copper proteins are characterized by an intense absorption ( $3\text{--}6\text{ mM}^{-1}\text{ cm}^{-1}$ ) at  $590\text{--}630\text{ nm}$  and by an unusually small  $A_{\parallel}$  value in their EPR spectra ( $\leq 90 \cdot 10^{-4}\text{ cm}^{-1}$ ) (Adman, 1991). These proteins are involved in electron transfer processes and exhibit relatively high midpoint potentials compared to the Cu(II)/Cu(I) aqua complex. Structural characterization of blue copper proteins including plastocyanin (Guss & Freeman, 1983; Guss et al., 1986), pseudoazurin (Petratos et al., 1988; Vakoufari et al., 1994), amicyanin (Durley et al., 1993; Kalverda et al., 1994; Romero et al., 1994), and azurin (Adman & Jensen, 1981; Baker, 1988; Nar et al., 1991a,b), indicates that the metal is bound by a strongly binding pseudotrigonal  $\text{N}_2\text{S}$  donor set derived from the side chains of two histidines and a cysteine. In azurin from *Pseudomonas aeruginosa*, these residues are His46, His117, and Cys112 (see Figure 1). In addition, there are two weakly interacting axial groups: Met121 and the carbonyl oxygen of Gly45. All other wild-type (wt)<sup>1</sup> blue copper proteins that have been structurally characterized so far have only a weakly interacting methionine at the axial position and lack

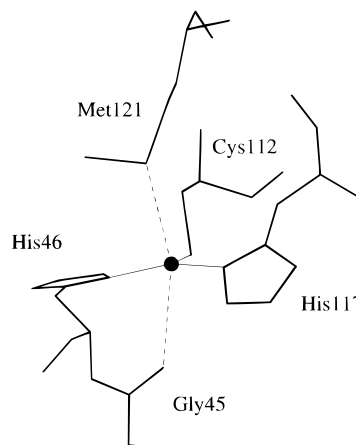


FIGURE 1: Schematic picture of the copper site of azurin from *Pseudomonas aeruginosa*.

the carbonyl oxygen. The distance of the Cu to the plane formed by the three strong ligands and the Cu–S(Met) bond length have been related to the rhombicity of the EPR spectrum and the ratio of the absorption bands at  $\sim 450$  and  $\sim 600\text{ nm}$  (Lu et al., 1993a; Han et al., 1993).

The application of site-directed mutagenesis techniques has added a new dimension to the study of metal sites in proteins, and blue copper proteins in particular. The role of the side chains that coordinate to the copper in the blue

<sup>†</sup> This research was supported in part by NATO Grants CRG 900603 and 930170 and NIH Grant GM-18865.

<sup>\*</sup> To whom correspondence should be addressed at Leiden Institute of Chemistry, Gorlaeus Laboratories, P.O. Box 9502, 2300 RA Leiden, The Netherlands. Telephone: +31 71 5274256. Fax: +31 71 5274349. Email: CANTERS@Rulga.LeidenUniv.nl.

<sup>‡</sup> Leiden University.

<sup>§</sup> Oregon Graduate Institute of Science and Technology.

<sup>||</sup> University of Oxford.

<sup>®</sup> Abstract published in *Advance ACS Abstracts*, January 1, 1996.

<sup>1</sup> Abbreviations:  $E$ , potential;  $E^0$ , midpoint potential; EDTA, (ethylenedinitrilo)tetraacetic acid; G, glycine; H, histidine; Hepes, 4-(2-hydroxyethyl)-1-piperazineethanesulfonic acid; IEF, isoelectric focusing;  $K_a$ , dissociation constant; Mes, 2-(*N*-morpholino)ethanesulfonic acid; NHE, normal hydrogen electrode; RR, resonance Raman; wt, wild-type.

copper proteins has been investigated by replacing each of them by a variety of residues (Karlsson et al., 1991; Mizoguchi et al., 1992; Romero et al., 1993; Germanas et al., 1993; Pascher et al., 1993; Kroes et al., 1993). A particularly intriguing modification appeared to be the replacement of ligand histidine-117 by a glycine (den Blaauwen et al., 1991, 1993; den Blaauwen & Canters, 1993). His117 protrudes slightly through the protein surface at the so-called hydrophobic patch, and the His to Gly mutation creates an aperture in this surface through which the Cu becomes directly accessible from the outside. This aperture can be filled by externally added ligands, and the original spectroscopic features of the Cu site can be restored by the addition of (substituted) imidazoles as ligands. Addition of other types of ligand results in Cu sites with so-called type-2 characteristics. This mutation, thus, has provided a versatile tool to modify the Cu site in a blue copper protein and study its properties. It appears that a similar modification can be applied in heme containing proteins with an axially ligating histidine. Replacing such a histidine by a glycine or an alanine creates a hole in the interior of the protein that can be filled with exogenous ligands (Barrick, 1994; McRee et al., 1994; Wilks et al., 1995). In a similar vein, the replacement of an axially ligating methionine by an alanine or even of an adjacent tryptophan by a glycine with the concomitant possibility of filling the internal hole in the protein structure by externally added residues has been reported (Lu et al., 1993b; Fitzgerald et al., 1994).

Recent structural studies by X-ray diffraction techniques (Hammann et al., 1996) have shown that the introduction of the His117Gly mutation considerably enhances the flexibility of the loop containing three of the four side chains (Cys112, His117, and Met121) that coordinate to the Cu in the wt azurin. This is expected to affect the malleability of the Cu site and the site's capacity to accommodate external ligands. It was thought important, therefore, to study a case by which, through a similar mutation, a hole next to the copper would be created that would be less flexible. For this purpose, His46 was replaced by a glycine. His46 is the second histidine ligand in the azurin Cu site, and it is the only ligand that is not present on the loop containing the other three ligands. It is located inside the protein, and its replacement by a glycine is expected to create a hole that is completely buried in the protein structure and the shape of which is sustained by an appreciably more rigid protein configuration than in the case of the His117Gly mutation. As mentioned above, such a modification was realized already in a number of heme-containing proteins, where it was used to great advantage in the study of the mechanistic properties of various cytochromes. A second reason to study the His46Gly mutant, therefore, was to check whether this type of modification is applicable to other classes of protein, like, in this case, blue copper proteins.

The location of His46 in the 3D azurin structure is illustrated in Figure 2, which presents a view perpendicular to the hydrophobic patch of azurin. Met13, -44, and -64 are shaded in dark grey, the other hydrophobic residues that make up this patch on the azurin surface are shaded light grey. The side chain of His117 is clearly visible in panel A of Figure 2, while His46 is covered and is invisible. In Figure 2B, Met44 has been removed, allowing the identification of His46 in the structure (dark grey). The hole that is

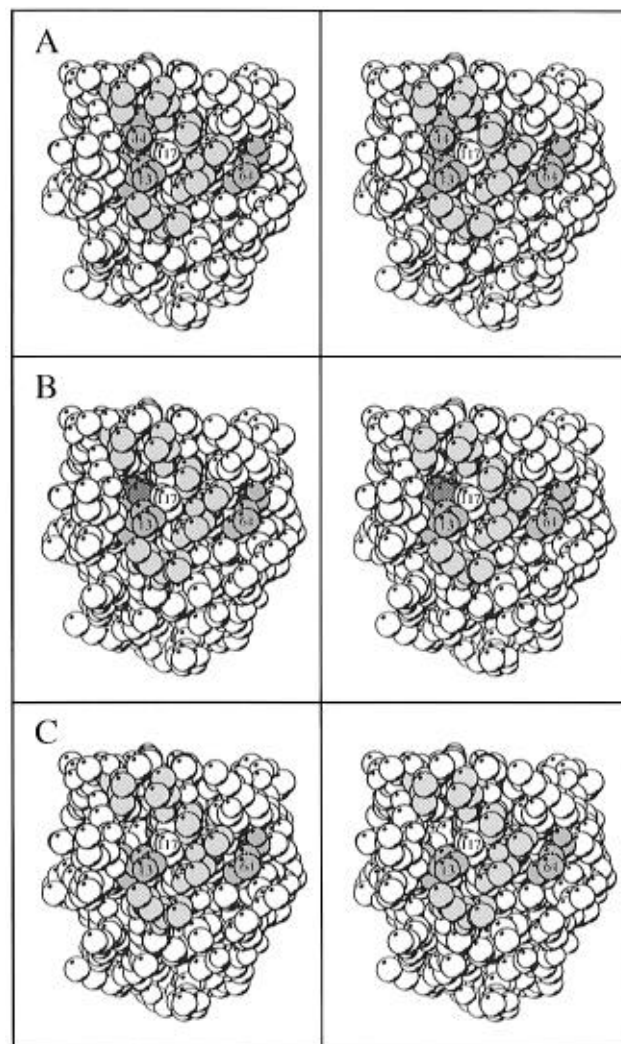


FIGURE 2: View perpendicular to the hydrophobic patch of azurin (Kraulis, 1991). The hydrophobic residues in this patch are colored light grey or intermediate grey (Nar et al., 1991a). (A) wt azurin; (B) wt azurin in which Met44 is removed to expose His46 (dark grey); (C) the same as (B) but with His46 replaced by Gly.

created when His46 is changed into a glycine is visible in Figure 2C. In practice, in the His46Gly mutant this hole will be covered by Met44.

Here we report on the preparation of the His46Gly mutant and the investigation of its properties by UV/vis, EPR, and resonance Raman (RR) spectroscopy. The mutated protein appears to exist either as a type-2 species or as an equilibrium mixture of type-1 and type-2 species, with the equilibrium constant depending on the ligand. The redox activity of the His46Gly mutant along with the kinetics of copper uptake have been compared with those of the His117Gly mutant. The absence of either His ligand increases the rate of copper uptake and yields a considerably more positive midpoint potential due to a stabilization of the Cu(I) state.

## EXPERIMENTAL PROCEDURES

**Bacterial Strains and Plasmids.** *E. coli* strain JM101 (Sambrook et al., 1989) was used for cloning and expression of the *Ps. aeruginosa* *azu* gene. The *azu* gene has been identified previously on a 1.3-kb chromosomal *Pst*I fragment which has been cloned into pUC18, resulting in plasmid pGC5 (Canters, 1987; van de Kamp et al., 1990a). Subsequently, in the plasmid pGC5, the *Sma*I site in the polylinker

was removed (van de Kamp, unpublished results). This resulted in the plasmid pGC13 which was used in the present study for the expression of the *azu* gene under the control of the *lac* promoter.

The His46Gly mutation was introduced in the *azu* gene with the use of the "Oligonucleotide-directed in vitro mutagenesis system" (Amersham). For this purpose, the 137 bp *Sall*–*XbaI* fragment of the plasmid pGC13 was cloned into M13mp19. A 16-mer deoxyribonucleotide primer was used to change the His46 codon CAC for the glycine codon GGC. The mutation was confirmed by sequencing the fragment as cloned in the M13 phage. Subsequently, the *Sall*–*XbaI* fragment of pGC13 was exchanged for the mutated fragment. The exchange was checked by again transferring the mutated fragment to M13mp19 and sequencing it. The plasmid containing the His117Gly mutation was described earlier (den Blaauwen et al., 1991). Recombinant DNA techniques were used according to standard protocols (Sambrook et al., 1989).

**Isolation of Apo-His46Gly and His117Gly Azurin.** His-117Gly azurin was isolated as described earlier (den Blaauwen & Canters, 1993).

His46Gly azurin was isolated from *E. coli* JM101 cells, transformed with the mutated plasmid pGC13. Cells were grown overnight and diluted 1:100 in 30 L of Luria–Bertani medium (Sambrook et al., 1989) supplemented with 100  $\mu$ g/mL ampicillin and 100  $\mu$ M isopropyl  $\beta$ -thiogalactopyranoside in a 40 L fermentor (MPP40; New Brunswick Scientific, Edison, NJ.). The cells were harvested immediately at the end of the exponential growth phase by filtration with a Pellicon cassette filter (Millipore Corp., Bedford, MA). The His46Gly azurin was isolated and purified as apo-protein, i.e., without addition of  $\text{Cu}^{2+}$  or potassium ferricyanide, but otherwise as described earlier (van de Kamp et al., 1990b). The apo-protein was pure as judged from IEF gel electrophoresis. The yield was 20 mg of purified protein per litre of cell culture.

**$^1\text{H}$ -NMR Spectroscopy.** NMR samples of apo-azurin were prepared by repeated concentration and dilution with  $\text{D}_2\text{O}$  in an Amicon ultrafiltration cell. The pH\*'s of the samples were adjusted by adding small amounts of 0.1 M DCl or 0.1 M NaOD to the protein solution (the asterisk indicates that the pH meter reading is not corrected for the deuterium isotope effect). The pH titration of apo-His46Gly azurin was performed in the same way as apo-wt azurin (van de Kamp et al., 1990b).

$^1\text{H}$ -NMR spectra were recorded on a Bruker WM-300 spectrometer at 298 K. The HDO resonance was suppressed by presaturation. Temperature calibration was achieved by recording the signal of tetramethylammonium nitrate. Free induction decays were accumulated in 8 K memory, deconvoluted by Gaussian multiplication, zero-filled to 16K data points, and Fourier-transformed.

**Reconstitution of the Apo-protein.** The concentration of the protein was determined from the absorbance at 280 nm. The assumption is made that the apo-His46Gly azurin has the same extinction coefficient at 280 nm as the wt Cu-azurin ( $9800 \text{ M}^{-1} \text{ cm}^{-1}$ ); 1–2 equiv  $\text{Cu}(\text{NO}_3)_2$  was added to a 0.1–1.0 mM solution of apo-protein in 20 mM Hepes, pH 7.5, upon which the solution immediately turned green. For the preparation of EPR samples and cyclic voltammetry samples, the Cu that was free in solution and the Cu that was nonspecifically bound to the protein were removed by a

repeated cycle of concentrating the protein solution and diluting it with buffer (20 mM Mes, pH 6.0, or 20 mM Hepes, pH 7.5) containing 1 mM EDTA in an Amicon ultrafiltration cell. This method was tested by incubating wt Zn-azurin with  $\text{Cu}^{2+}$ . This solution was subsequently treated with buffer containing 1 mM EDTA in the manner described above, and an EPR spectrum was recorded. No significant  $\text{Cu}^{2+}$  signal could be detected (results not shown). We conclude that treatment with 1 mM EDTA removes most or all of the nonspecifically bound copper.

**Ligands.** KBr, sodium acetate, sodium formate,  $\text{KNO}_3$ , and *N*-propylamine were purchased from E. Merck AG, Darmstadt, Germany; 4-methylimidazole, 4-methylthiazole and thiazole were purchased from Janssen Chimica, Beerse, Belgium; *N*-butylimidazole was purchased from Fluka AG, Bluchs, Switzerland; other ligands were purchased from the sources described in den Blaauwen and Canters (1993).

**UV/vis Spectroscopy.** UV/vis experiments were performed on a 0.1 mM reconstituted protein solution in a cuvette with a 1-cm path length. In the pH titration experiments, the pH was changed by adding aliquots of 0.1–1 M NaOH or 0.1–1 M  $\text{HClO}_4$ . The room temperature (298 K) measurements were done on a Philips PU8745 or a Shimadzu UV-2101PC UV/vis spectrophotometer, the 77 K measurements on an Aminco-Chance DW-2 spectrophotometer.

For determination of the dissociation constant ( $K_d$ ) a 0.1 mM azurin solution of reconstituted His46Gly in 100 mM Hepes, pH 7.5, or 20 mM Mes, pH 6.0, was titrated with concentrated ligand solution. The  $K_d$  and the absorbance at infinite ligand concentration ( $A^\infty$ ) were determined from the fit of the absorbance,  $A(L)$ , as a function of the concentration of added ligand ( $[L]$ ) according to the equation:

$$A(L) = A^0 + [L](A^\infty - A^0)/(K_d + [L]) \quad (1)$$

in which  $A^0$  is the absorption at ligand concentration 0. The absorbance was measured at wavelengths where the largest changes occur upon adding ligand. Only spectral traces that pass through the isosbestic point(s) were used for determination of the  $K_d$  and  $A^\infty$ . The absorbances of the bands at infinite ligand concentration are quoted as the percentage of the absorbance at 280 nm for the apo-protein.

**EPR Spectroscopy.** EPR spectra were recorded with a JEOL JESRE2X spectrometer operating at X-band frequency and interfaced with a JEOL ES-PRIT330 data manipulation system. Parameters for recording the EPR spectra were typically 16.7 mT/min sweep rate, 0.8 mT modulation amplitude, 9.0 GHz frequency, and 5 mW incident microwave power. The magnetic field was calibrated with an external sample of  $\alpha, \alpha'$ -diphenyl- $\beta$ -picrylhydrazyl. Protein samples contained 2 mM Cu(II) protein.

**Resonance Raman Spectroscopy.** Samples for RR measurements (4 mM protein in 50 mM buffer) were prepared from solutions of apo-His46Gly azurin in water (16  $\mu\text{L}$ , 5 mM) by the addition of 1  $\mu\text{L}$  of the desired buffer (1 M Hepes, pH 7.5, or 1 M Mes, pH 5.5), followed by 0.8  $\mu\text{L}$  of 0.1 M  $\text{Cu}(\text{NO}_3)_2$  solution and finally 2  $\mu\text{L}$  of 10 times concentrated ligand solution or 2  $\mu\text{L}$  of water. The following ligands were added to the protein at pH 7.5 (final concentrations in parentheses): sodium acetate (0.25 M), 2-methylimidazole (0.1 M), imidazole (25 mM), *N*-methylimidazole (25 mM), KSCN (20 mM), and histamine (10 mM). The final pH of the protein sample was checked using an MI-

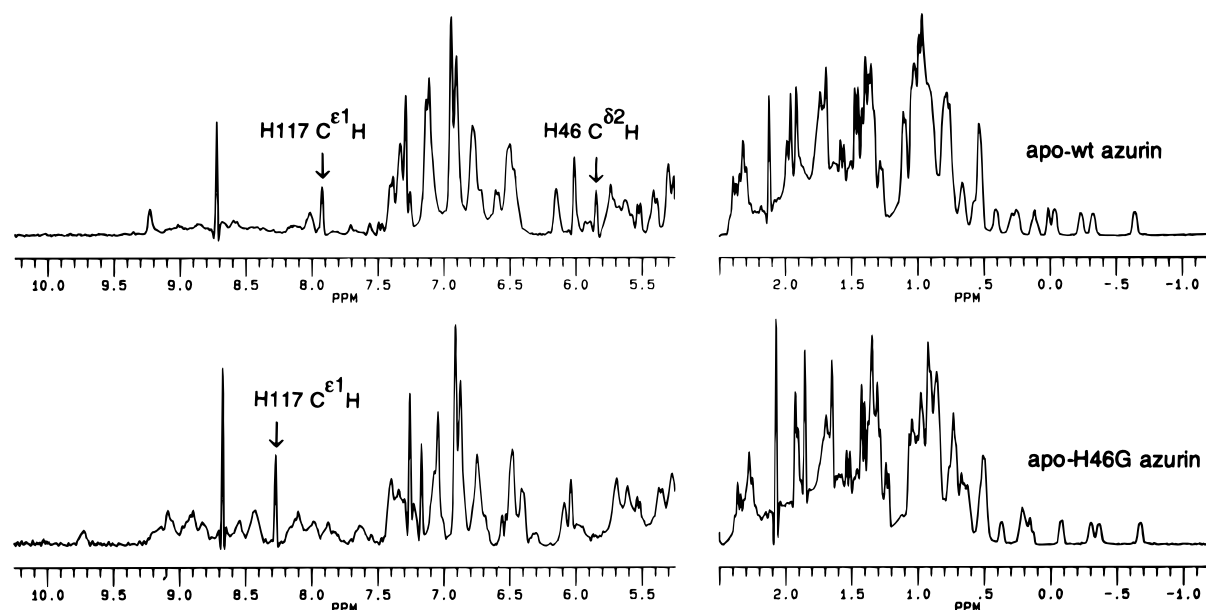


FIGURE 3: Room temperature  $^1\text{H}$ -NMR spectra of apo-wt (20 mM  $\text{K}_2\text{DPO}_4/\text{KD}_2\text{PO}_4$  buffer, pH\* 5.0) and apo-His46Gly ( $\text{D}_2\text{O}$ , pH\* 5.0) azurin. Protein concentrations amounted to 3 mM.

410 electrode (Microelectrodes, Inc.) attached to a pH meter. When the pH changed by more than 0.5 pH units, the pH was adjusted by the addition of 1  $\mu\text{L}$  aliquots of 0.1 M NaOH or 0.1 M  $\text{HNO}_3$  solution. NaCl was added to a pH 5.5 protein solution to give a final concentration of 0.5 M. Samples were checked prior to the RR experiments by recording their room temperature UV/vis spectra.

Raman spectra were obtained on a Jarrell-Ash 25–300 spectrophotometer, equipped with an Ortec Model 9302 amplifier/discriminator and an RCA C31034 photomultiplier, and interfaced to an Intel 310 computer. The desired excitation wavelengths were provided by the following lasers: Spectra-Physics 2025–11 Kr, Spectra-Physics 164 Ar, and Coherent Innova 90–6 Ar. Raman spectra were recorded at 0.5  $\text{cm}^{-1}/\text{s}$  in an  $\sim 150^\circ$  back-scattering geometry from samples maintained at 15 K using a closed-cycle helium refrigerator (Air Products Displex) and in capillaries maintained at 90 K (liquid  $\text{N}_2$  cooling). For liquid samples at 278 K (ice-cooling), a  $90^\circ$  scattering geometry was used. Absolute frequencies are accurate to  $\pm 1 \text{ cm}^{-1}$ .

**Rate of  $\text{Cu}^{2+}$  Binding.** Stopped-flow kinetic experiments were performed at 293 K by using a Hi Tech Scientific stopped-flow apparatus (Hi Tech Scientific PQ/SF-53, spectrophotometer unit SU-40, photomultiplier PSU PPS-60) equipped with a 1-cm path length observation chamber (dead time 5 ms). A 50  $\mu\text{M}$  apo-protein solution in 20 mM Mes, pH 6.0, was mixed with a 1.0, 2.0, or 4.0 mM  $\text{Cu}(\text{NO}_3)_2$  solution in 20 mM Mes, pH 6.0. The reactions were monitored at the wavelengths of the maximum absorbances of the copper proteins: at 400 nm for His46Gly, at 420 and 628 nm for His117Gly, and at 628 nm for wt azurin. Absorbance changes were analyzed as a function of time by using a fitting procedure for first-order reactions (A. Braat, Technical University of Delft).

**Reconstruction of Reduced His46Gly and His117Gly Azurin.** His46Gly, His117Gly, and wt azurin were reduced with a slight excess of ascorbic acid or dithionite. Back-oxidation was tried with  $\text{K}_3\text{Fe}(\text{CN})_6$  and ammonium peroxydisulfate. Copper was removed from reduced His46Gly and His117Gly azurin by overnight incubation of the protein

in a solution containing 0.1 M thiourea, 0.1 M Mes, 1 mM EDTA, and 0.25 M NaCl, pH 5 (Blaszak et al., 1983), followed by thorough rinsing with 0.1 M Mes, pH 6, in an Amicon ultrafiltration cell. After addition of 0.5 M NaCl to this solution, it was used for Cu reconstitution experiments. Reconstitution was studied by watching the growth of the absorption band around 630 nm after addition of 1–2 equivalents of  $\text{Cu}(\text{NO}_3)_2$  to the solution.

**Electrochemical Measurements.** Cyclic (linear sweep) voltammetry was performed at an edge-plane graphite electrode arranged in a 1 mL three-electrode, two-compartment glass cell. A saturated calomel reference electrode was inserted into the reference side-arm which was connected by a 0.1 mm Luggin capillary to the working compartment, containing a platinum–gauze counter-electrode. A pH electrode was inserted in the working compartment to measure the pH between the measurements. The buffer solution was 100 mM Hepes, 0.3 M KCl, or 0.15 M  $\text{KNO}_3$ , pH 7.4, in Milli-Q water. Concentrated protein was added to provide a concentration of 0.5 mM. The voltammograms were recorded at several pH values. The pH was changed by adding 1.0 M HCl or  $\text{HNO}_3$  solution to the working compartment. The potential was controlled by an Ursar Scientific Instruments (Oxford) potentiostat, and voltammograms in the range 50–850 mV (normal hydrogen electrode) were recorded on a Gould series 60000 chart recorder. The scan rate was 20 mV/s. The electrode was polished before use with a 0.3  $\mu\text{m}$  alumina/water slurry and sonicated briefly, followed by thorough rinsing with water.

## RESULTS

**NMR Spectroscopy.** The 300 MHz NMR spectra of apo-wt and apo-His46Gly azurin are displayed in Figure 3. The absence of several NH resonances in the 7.5–10 ppm region of the wt azurin spectrum is due to a longer incubation of the wt protein in  $\text{D}_2\text{O}$  compared to His46Gly azurin. This has promoted the exchange of the amide protons with the deuterons of the solvent.

**His46Gly( $\text{H}_2\text{O}$ ): Optical Spectra.**  $\text{Cu}^{2+}$ , when added to a solution of the colorless His46Gly apo-protein, reacts

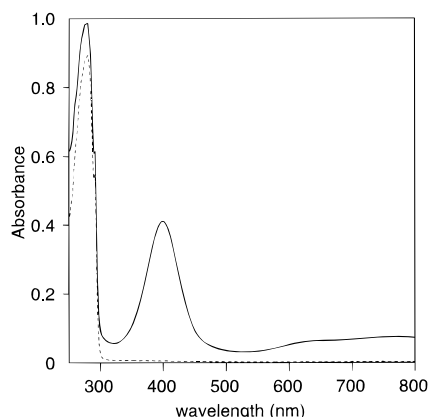


FIGURE 4: Room temperature electronic absorption spectra of 0.1 mM apo-His46Gly (dotted line) and reconstituted His46Gly azurin (solid line) in 20 mM Hepes, pH 7.5. Path length, 1 cm.

instantaneously with the protein, as can be seen from the development of a green color. The reaction is completed within seconds. Adding more than 1 equiv of copper does not lead to any further increase in absorption. The green color of the solution is due to a strong optical absorption band at 400 nm and two weak bands around 630 and 760 nm (see Figure 4). The extinction coefficient at 400 nm [calculated from a comparison with the 280 nm absorbance (see Experimental Procedures)] is  $4500 (\pm 200) \text{ M}^{-1} \text{ cm}^{-1}$ .

Between pH 8.5 and 6.5, the spectrum is pH-independent. Below pH 6.5, the intensity of the band at 400 nm decreases slightly, while the 630 nm band increases somewhat in intensity. Below pH 5 and above pH 8.5, both bands bleach irreversibly.

**His46Gly with External Ligands: Optical Spectra.** When exogenous ligands are added to the reconstituted protein, the absorption spectrum changes. Examples are shown in Figure 5. A common observation is that upon the addition of ligand the 400 nm band decreases and one or more other absorption bands appear. Sometimes the 400 nm band is replaced by two new bands at a longer wavelength (Figure 5a–d); in other cases, a single new band appears at a shorter wavelength (Figure 5e,f). Often isosbestic behavior is observed

(Figures 5a,b,d,f). When more than one new band arises, the intensities of the new bands are in constant proportion independent of the ligand concentration. The results are summarized in Table 1.

For ligands with or without an imidazole group, the  $K_d$  increases or decreases, respectively, when the pH is lowered from 7.5 to 5.5. Addition of histidine, thiazole, 4-methylthiazole, *N*-polyvinylimidazole, *N*-propylamine, and *N*<sup>ω</sup>-acetylhistamine has no effect on the absorption spectrum, except that the bands gradually lose intensity in the course of a titration. From this, we conclude that these ligands do not bind to the  $\text{Cu}^{2+}$  in the protein, but rather compete with the protein for  $\text{Cu}^{2+}$  and gradually extract the metal out of the His46Gly azurin.

**EPR Spectroscopy.** The EPR spectrum of reconstituted His46Gly azurin [His46Gly( $\text{H}_2\text{O}$ )] (treated with 1 mM EDTA to remove nonspecifically bound  $\text{Cu}^{2+}$ ) is shown in Figure 6a. The main species detected by EPR has type-2 Cu site characteristics (Vännegård, 1972; Peisach & Blumberg, 1974) with  $A_{\parallel} = 160 (\pm 10) \times 10^{-4} \text{ cm}^{-1}$  and  $g_{\parallel} = 2.24 (\pm 0.01)$ . The spectrum is pH-independent in the range pH 6–8.5 and has a rhombic appearance although the splitting in the  $g_{\perp}$  region might be due to other species present in lower concentrations. The peaks in the  $g_{\parallel}$  region show some super-hyperfine splitting which is clearly visible in the most downfield-shifted hyperfine line. The magnitude of the splitting ( $\sim 13 \text{ G}$ ) is compatible with a magnetic interaction with at least one nitrogen nucleus.

The EPR spectra of reconstituted His46Gly azurin in 0.5 M NaCl in the presence and absence of 40% glycerol at 77 K are shown in Figure 6b,c, respectively. Trace 6b corresponds to a type-2 Cu site. Only in the absence of glycerol, a major type-1 spectrum is obtained at 77 K (Figure 6c) with  $g_{\parallel} = 2.29 (\pm 0.02)$  and  $A_{\parallel} \leq 30 \times 10^{-4} \text{ cm}^{-1}$ . The positions these species occupy in a Vännegård–Blumberg–Peisach plot (Vännegård, 1972; Peisach & Blumberg, 1974) are illustrated by Figure 7, which for comparison also contains data points obtained for His117Gly azurin with various exogenous ligands (den Blaauwen & Canters, 1993).

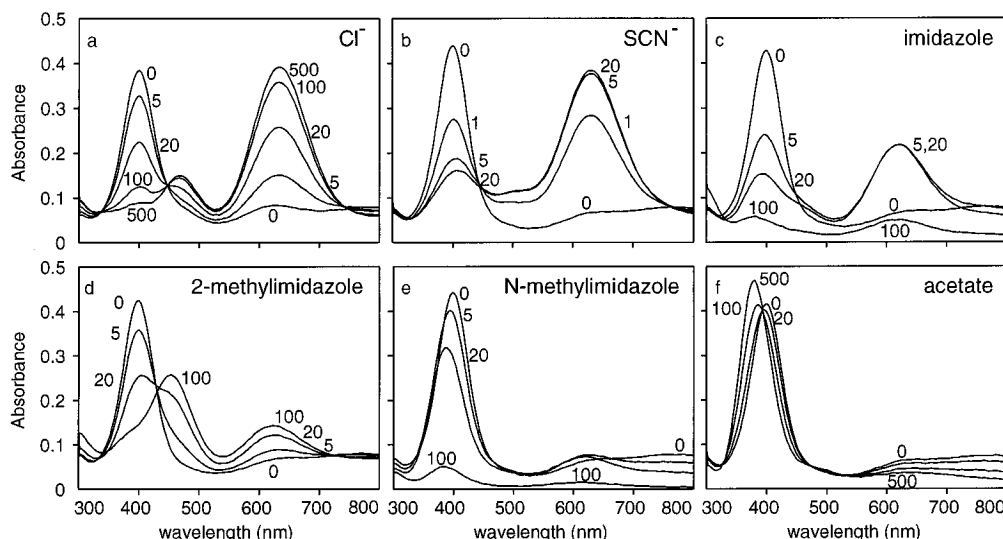


FIGURE 5: Titrations of 0.1 mM reconstituted His46Gly azurin (a) in 20 mM Mes, pH 6.0, with a 5.0 M NaCl solution; (b) in 100 mM Hepes, pH 7.5, with a 1.0 M KSCN solution; (c) in 100 mM Hepes, pH 7.5, with a 1.0 M imidazole solution; (d) in 100 mM Hepes, pH 7.5, with a 1.0 M 2-methylimidazole solution; (e) in 100 mM Hepes, pH 7.5, with a 1.0 M *N*-methylimidazole solution; (f) in 100 mM Hepes, pH 7.5, with a 1.0 M sodium acetate solution. The numbers in the figures indicate the ligand concentration in millimolar.

Table 1: UV/vis Parameters and Dissociation Constants of His46Gly Azurin with Exogenous Ligands<sup>a</sup>

ligand	$\lambda_{\max}^b$	$\lambda_{\max}^b$	$\lambda_{\max}^b$	isosbestic points (nm)			$K_d^c$
wild-type		481(2)	628(58)				
OH <sup>-</sup> /H <sub>2</sub> O	400(45)		630(7), 760(8)				
Cl <sup>-</sup>		469(17)	634(43)	337	447	744	16 mM (pH 6.0)
Br <sup>-</sup>	320(11), 396(13)	489(14)	659(45)	346	457	780	16 mM (pH 6.0)
SCN <sup>-</sup>	405(15)	500(9)	630(45)		450	770	0.80 mM
N <sub>3</sub> <sup>-</sup>	405(17)		651(55)		438		2.0 mM
imidazole	380(17)		621(32)		450		2.7 mM
4-methylimidazole	395(17)		625(27)		442		1.7 mM
2-methylimidazole		452(34)	621(17)		430	712	20 mM
N-methylimidazole	385(32)		621(8)	383		655	9 mM
N-butylimidazole	385(50)		621(7)	395	464	639	4 mM
CH <sub>3</sub> COO <sup>-</sup>	377(54)			393			0.10 M
HCOO <sup>-</sup>	384(49)			395			0.25 M
NO <sub>3</sub> <sup>-</sup>	388(51)			399			37 mM (pH 6.0)
histamine	378(63)			386	494	556	0.86 mM

<sup>a</sup> The estimated errors in the  $K_d$  and the percentage of the 280 nm absorption are 20%. <sup>b</sup> Wavelength in nanometers of maximum absorbance. In parentheses, the absorption, extrapolated to infinite ligand concentration, is indicated as a percentage of the 280 nm absorption of apo-His46Gly azurin. <sup>c</sup> Dissociation constant of His46Gly azurin and ligand at pH 7.5, unless indicated otherwise.

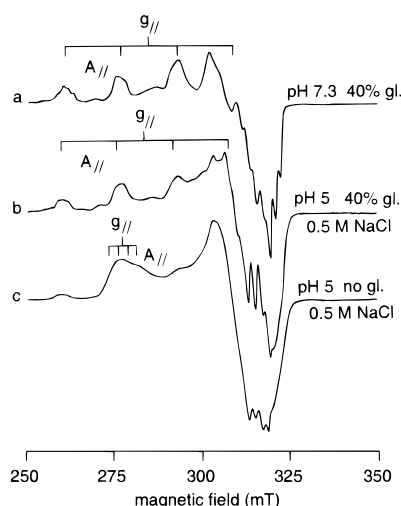


FIGURE 6: EPR spectra of 2 mM reconstituted His46Gly azurin at 77 K (a) in 10 mM Hepes, 40% glycerol, pH 7.3; (b) in 0.5 M NaCl, 40% glycerol, pH 5; (c) in 0.5 M NaCl, pH 5.

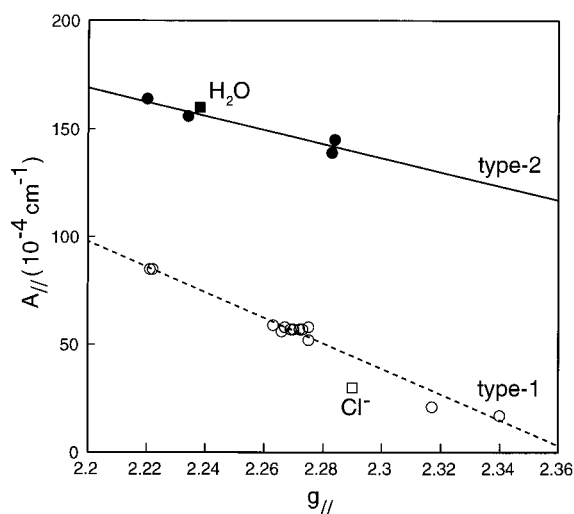


FIGURE 7: Plot of  $A_{||}$  vs  $g_{||}$  of His46Gly(H<sub>2</sub>O) (■) and His46Gly(Cl<sup>-</sup>) (□). Other points refer to type-1 variants (○) and type-2 variants (●) of His117Gly azurin [data taken from den Blaauwen and Canters, (1993)].

**UV/vis Spectroscopy at 77 K.** UV/vis spectra of reconstituted His46Gly azurin in 0.5 M NaCl, pH 5.0 at 77 K, in the presence and absence of 40% glycerol are shown in

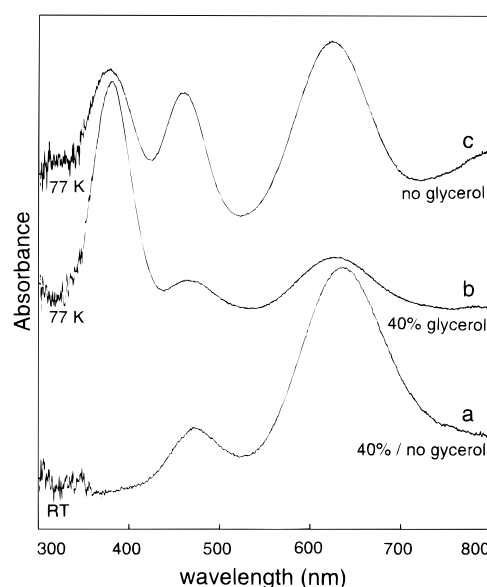


FIGURE 8: Electronic absorption spectrum of reconstituted His46Gly azurin in 0.5 M NaCl, pH 5, (a) at room temperature in the absence of glycerol (the spectrum in the presence of 40% glycerol is identical to the one shown); (b) in the presence of 40% glycerol at 77 K; (c) in the absence of glycerol at 77 K.

Figure 8b,c, respectively. The increased absorbance at 469 and 634 nm in the absence of glycerol (Figure 8c) corresponds to the type-1 species seen in the EPR spectrum (Figure 6c). They differ from the room temperature spectra, which are independent of the glycerol concentration and lack the band around 400 nm (Figure 8a). This band is characteristic of the chloride-free (type-2) species, and at 77 K it is present at about 380 nm. Apparently, lowering the temperature increases the  $K_d$  of the Cl<sup>-</sup> dissociation equilibrium.

**Resonance Raman Spectroscopy.** (A) His46Gly Azurin in Water. Excitation within the minor absorption band around 630 nm (see Figure 4) using 647 nm gives a RR spectrum with maximum intensity at 394 cm<sup>-1</sup> (see Figure 9A), typical of the trigonal coordination of a type-1 site with a slight rhombic distortion (Andrew et al., 1994). Excitation at 413 nm gives a different RR spectrum as depicted in Figure 9B. The occurrence of the most intense band at 330 cm<sup>-1</sup> is consistent with a type-2 coordination of the Cu by four strong

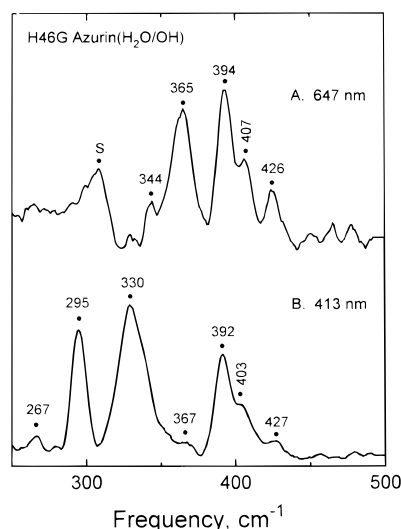


FIGURE 9: Resonance Raman spectra of His46Gly azurin (no ligand added). Spectra were obtained at 90 K from 4 mM protein in 20 mM Hepes, pH 7.5 (A), using 647.1 nm (80 mW) and (B) 413.1 nm (35 mW) excitations with a resolution of 5.0  $\text{cm}^{-1}$ , scan rate of 0.5  $\text{cm}^{-1}/\text{s}$ , and accumulation of 4 scans per spectrum. S indicates a solvent peak.

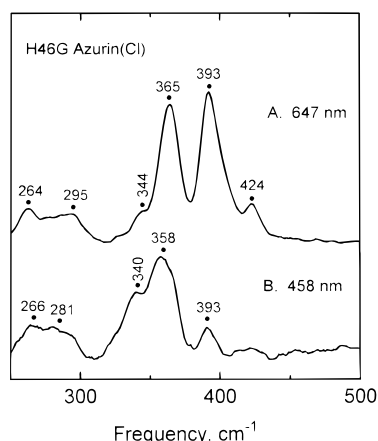


FIGURE 10: Resonance Raman spectra of His46Gly azurin plus 0.5 M chloride. Spectra were obtained from 4 mM protein in 20 mM Mes, pH 5.5, using (A) 647.1 nm and (B) 457.9 nm excitation ( $\sim 30$  mW) with a resolution of 5.0 and 8.0  $\text{cm}^{-1}$ , respectively, scan rate of 0.5  $\text{cm}^{-1}/\text{s}$ , and accumulation of 2–4 scans per spectrum.

ligands (Andrew et al., 1994). There was no difference in RR peak positions when samples were measured at 15, 90, or 278 K.

(B) *His46Gly Azurin with  $\text{Cl}^-$* . With  $\text{Cl}^-$  as a ligand, excitation at 647 nm (see Figure 5a) gives a RR spectrum (see Figure 10A) at 278 K with maximum intensity at 393  $\text{cm}^{-1}$ , typical of a type-1 site with slight rhombic distortion. Excitation at 458 nm within the 469 nm band results in a different RR spectrum with maximum intensity at 358  $\text{cm}^{-1}$  (see Figure 10B).

(C) *His46Gly Azurin with  $\text{SCN}^-$ , Imidazole, 2-Methylimidazole, or N-Methylimidazole*. Excitation within the  $\sim 600$  nm absorption bands (see Figure 5b–e) leads to RR spectra typical of a type-1 species with the most intense RR band between 393 and 408  $\text{cm}^{-1}$  (Table 2). The occurrence of the most intense RR band near 408  $\text{cm}^{-1}$  (imidazole and 2-methylimidazole) signifies a trigonal planar ligand set with an axial geometry, whereas main bands with frequencies between 400 and 393  $\text{cm}^{-1}$  (N-methylimidazole and  $\text{SCN}^-$ )

are typical of rhombic type-1 sites with a slight tetrahedral distortion. Excitation within the  $\sim 400$  nm absorption band leads to a RR spectrum typical of a type-2 species with the most intense RR band between 325 and 328  $\text{cm}^{-1}$  (Table 2) (Andrew et al., 1994).

(D) *His46Gly Azurin with Histamine or Acetate*. In both cases, no evidence for a type-1 RR spectrum is observed at 647 nm excitation (see Figure 5f), and only a typical type-2 RR spectrum is observed when excitation is performed at 413 nm. Apparently, the equilibrium between the type-1 and type-2 sites lies far in favor of the type-2 center.

*Rate of Cu Binding*. When excess  $\text{Cu}^{2+}$  is added to a solution of the apo-protein, the absorbance changes of wt and His46Gly azurin follow pseudo-first-order kinetics. The observed pseudo-first-order rate constants are given in Table 3. The absorbance changes of His117Gly at 420 and 628 nm are biphasic. The two phases each comprise about half of the total absorption increase at both the monitored wavelengths. Only the observed rate constant for the fast phase is given in Table 3. The slow phase has a rate constant of 0.02 ( $\pm 0.01$ )  $\text{s}^{-1}$ , independent of  $\text{Cu}^{2+}$  concentration.

*$pK_a$  of His117 in His46Gly Azurin by  $^1\text{H-NMR}$  Spectroscopy*. For the apo-wt azurin at pH\* 5.0, the resonance position of the  $\text{C}^\epsilon\text{H}$  proton of His117 occurs at 7.92 ppm (Figure 3, upper). In the apo-His46Gly azurin, this resonance is missing. Instead, there is a new sharp resonance at 8.30 ppm at pH\* 5.0, the position of which is pH-dependent (Figure 3, lower). This resonance is ascribed to the His117  $\text{C}^\epsilon\text{H}$  proton of the apo-His46Gly azurin. Its  $pK_a$  was determined from a pH titration and amounts to  $6.6 \pm 0.2$  as opposed to 7.6 in wt apo-azurin (van de Kamp et al., 1990b).

*Reconstruction of His46Gly and His117Gly Azurin after Reduction*. The green color of the reconstituted His46Gly or His117Gly azurin disappears upon reduction with ascorbate within seconds. Complete reduction of wt azurin under the same conditions takes at least 1 h. The wt protein can be oxidized back with both  $\text{K}_3\text{Fe}(\text{CN})_6$  and ammonium peroxydisulfate. Back-oxidation of reduced His46Gly or His117Gly azurin in this manner appears impossible [0.1 mM protein in 20 mM Hepes, pH 7.5, or 20 mM Mes, pH 6.0, at 298 K with 1–10 equiv of  $\text{K}_3\text{Fe}(\text{CN})_6$  or ammonium peroxydisulfate]. Adding extra  $\text{Cu}^{2+}$  to the reduced His46Gly or His117Gly azurin solution does not restore the color. Slow back-oxidation with ammonium peroxydisulfate is possible, however, in the presence of excess chloride: after 1 h, about 60% of the absorbance around 630 nm is recovered in the presence of 0.5 M NaCl.

Treatment of reduced His46Gly or His117Gly azurin with thiourea, which is expected to remove the metal from the Cu binding site (Blaszak et al., 1983), results in protein that can be reconstituted up to 90% by adding  $\text{Cu}^{2+}$ .

*Electrochemical Measurements*. The His46Gly and His117Gly azurins gave a quasi-reversible electrochemical response at an edge-plane graphite electrode in the presence of 0.3 M KCl. The cyclic voltammograms at several pHs are shown in Figure 11. The His46Gly azurin gave a better response than the His117Gly azurin. The results obtained from the cyclic voltammograms are given in Table 4. In the absence of  $\text{Cl}^-$  neither His46Gly nor His117Gly azurin gave any electrochemical response in the voltage range 50–850 mV (normal hydrogen electrode;  $\text{KNO}_3$  as supporting electrolyte), although the His117Gly mutant appeared to exhibit a weak reductive wave.

Table 2: Resonance Raman Spectra of His46Gly Azurin with Externally Added Ligands

ligand	excitation (nm)	resonance Raman peak positions (cm <sup>-1</sup> ) <sup>a</sup>									
Type-1 Cu site											
OH <sup>-</sup> /H <sub>2</sub> O (pH 7.5)	647				344	365	<b>394</b>	407	426		
Cl <sup>-</sup>	647	264		295		365	<b>393</b>		424		
SCN <sup>-</sup>	647	263	279	296	346	369	<b>397</b>	406	423		476
imidazole	647	263	279		346	369	397	<b>408</b>	427	455	475
2-methylimidazole	647	254			345	369	400	<b>406</b>	425		
N-methylimidazole	647				345	363	<b>393</b>	409	424		
Type-2 Cu site											
Cl <sup>-</sup>	458	266	281		340	<b>358</b>		393			
2-methylimidazole	458	268		295	<b>327</b>	348		391			
OH <sup>-</sup> /H <sub>2</sub> O (pH 7.5)	413	267		295	<b>330</b>	339		392	403	427	
SCN <sup>-</sup>	413	270		293	<b>327</b>	340	346	390	400	425	461
imidazole	413	261		295	<b>325</b>	337	353	388		426	
N-methylimidazole	413	262		297	<b>328</b>	340	352	387		427	
CH <sub>3</sub> COO <sup>-</sup>	413	262		<b>293</b>		<b>340</b>	355	390		424	
histamine	413	259		299	<b>335</b>	344		394			

<sup>a</sup> Boldface denotes most intense RR peak. RR spectral conditions as in Figure 7. Samples at 278 K except for imidazole and N-methylimidazole complexes at 15 K.

Table 3: Observed Pseudo-First-Order Rate Constants in s<sup>-1</sup> for Cu Uptake by Apo-protein<sup>a</sup>

protein	wavelength (nm)	1 mM Cu <sup>2+</sup>	2 mM Cu <sup>2+</sup>	4 mM Cu <sup>2+</sup>
H46G	400	2.3	3.5	6.6
H117G	420	0.6	1.0	1.3
H117G	628	0.4	0.7	1.1
wt <sup>b</sup>	628	0.073	0.16	0.34

<sup>a</sup> Experimental conditions: 50 μM apo-protein in 20 mM Mes buffer, pH 6.0, at 293 K. The estimated error in the observed rate constants is 15%. <sup>b</sup> No difference was observed between wt apo-protein made by treatment of Cu protein with KCN (Yamanaka et al., 1963) or thiourea (Blaszak et al., 1983).

Table 4: Midpoint Potentials of the His46Gly and H117G Azurins with Cl<sup>-</sup> as Ligand

protein	pH	Δ (mV) <sup>a</sup>	E <sup>0</sup> (mV) <sup>b</sup>	E <sup>0</sup> (wt) (mV) <sup>c</sup>
H46G	7.4	190	345	313
H46G	5.9	85	416	346
H46G	4.7	85	452	362
H117G	6.0	140	433	344
H117G	4.7	165	472	362
H117G	3.7	145	500	374

<sup>a</sup> Δ denotes the distance in millivolts between the oxidation and reduction wave. <sup>b</sup> Midpoint potential relative to the normal hydrogen electrode. <sup>c</sup> wt midpoint potentials (van Pouderoyen et al., 1994). The estimated errors in Δ and E<sup>0</sup> are 5–10 mV.

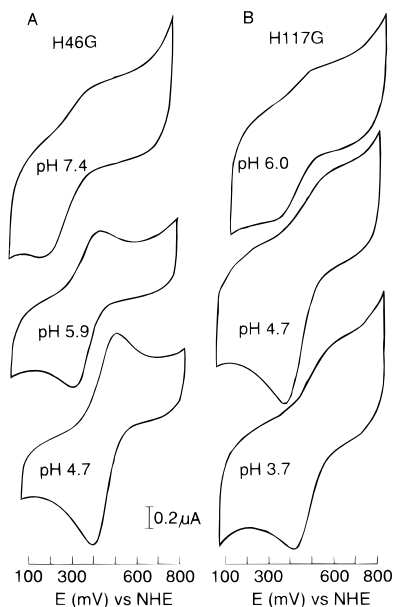


FIGURE 11: Cyclic voltammograms of (A) His46Gly and (B) His117Gly azurin in 0.1 M Hepes, 0.3 M KCl at several pHs.

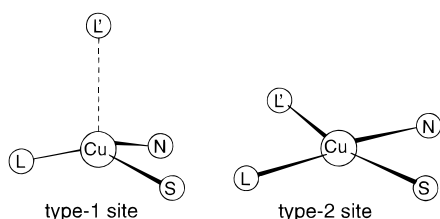
## DISCUSSION

**Protein Structure.** A global impression of the effect that the introduction of the His46Gly mutation has on the protein's structure can be gleaned from Figure 3, where the 300 MHz NMR spectra of the apo-forms of His46Gly and wt azurin are compared. As pointed out above, the differences in the 7.5–10 ppm regions between the two spectra are related to the different extents by which the backbone

amide protons have exchanged with the solvent (D<sub>2</sub>O). However, the other regions of the spectrum are suited for a comparison. The 0.5 to –1.0 ppm region contains the ring current shifted resonances, which are known to be sensitive indicators of structural differences. In general, variations in atomic positions on the order of 0.1 Å clearly show up as variations in the positions of these upfield-shifted resonances. The similarity between the two spectra in this region is an indication, therefore, for similar 3D structures. The second comparison comprises the region from 2.2 to 1.5 ppm, which contains most of the methionine ε-CH<sub>3</sub> signals. Also here the similarity between the two spectra is striking. The region in between (1.5–0.5 ppm) contains mainly resonances from aliphatic side chains, and although small variations in the spectrum are visible, the overall impression is again that of substantial likeness. In the fingerprint region of the spectrum extending from 5 to 6.3 ppm, there are differences which to a large extent can be ascribed to the absence of His46 in the His46Gly azurin. The differences between the two spectra in the aromatic region, from 6.3 to 8.0 ppm, primarily concern singlet signals at 7.9 and around 7.2 ppm. The differences can be ascribed to small differences in the titrating behavior of a number of histidines. Although a much more elaborate analysis of the spectrum of the mutant protein would be needed [the wt spectrum has been analyzed thoroughly, already (van de Kamp et al., 1992)] in order to make a definitive statement about the structural differences between the two proteins, the overall picture emerging from the comparison is that if there are structural differences, they must be small and be confined to the region around His46.



Scheme 1



This conclusion is fully substantiated by a recent crystallographic study of a number of azurin mutants, including apo-His46Gly (Hammann et al., 1996). The conclusions from that work, which are relevant for the present study, are that the 3D structures of the apo-wt (Nar et al., 1992) and the apo-His46Gly azurin are virtually identical (rms difference between C $\alpha$ -positions 0.4 Å, and between all heavy atom positions 0.7 Å) and that the cavity created by the His46Gly replacement is maintained in the structure of the mutated protein. An immobilized water molecule can be identified in the density map of the apo-His46Gly azurin, approximately at the position where the His46N $\delta$  atom occurs in the wt structure. An additional water molecule is seen in the structure of apo-His46Gly at the position occupied by the Cu in the wt structure. Thus, it can be concluded that, apart from the mutated side chain at position 46, the structure of the His46Gly azurin is virtually unperturbed by the mutation and that at position 46 there is an internal cavity in the protein structure that is accessible for water.

**His46Gly(H<sub>2</sub>O).** The immediate appearance of a strong optical absorption upon addition of Cu<sup>2+</sup> to a solution of the apo-His46Gly azurin shows that the metal site is restored. For brevity, this species (in the absence of externally added ligands) is denoted by His46Gly(H<sub>2</sub>O). The position of the strong absorption at 400 nm is typical of a type-2 Cu–cysteinate coordination (Andrew et al., 1994), and the appearance of a 15 G superhyperfine splitting in the EPR spectrum of this species, which in the case of the wt protein has been identified as being due to the interaction of the unpaired spin with the N $\delta$  of a ligand histidine, is compatible with His117 binding to the Cu.

The RR results confirm this conclusion. RR spectroscopy has proved particularly useful for distinguishing between different coordination geometries of copper–cysteinate sites because it is a sensitive indicator of changes in Cu–S(Cys) bond length (Andrew et al., 1994). Type-1 copper sites with three strong ligands in a distorted trigonal planar array (Scheme 1) exhibit their predominant Cu–S(Cys) stretching vibration,  $\nu(\text{Cu–S})$ , at 355–405 cm<sup>–1</sup>. Type-2 copper–cysteinate sites with four strong ligands in a tetragonal array (Scheme 1) have longer Cu–S(Cys) bond lengths, and their principal  $\nu(\text{Cu–S})$  modes are observed at 300–340 cm<sup>–1</sup>.

The RR experiments on the His46Gly(H<sub>2</sub>O) azurin solutions (Figure 9) show that the 430 and 630 nm bands in the optical spectrum correspond with a four-coordinated type-2 site, and a trigonal type-1 site with a slight rhombic distortion, respectively. As one of the strong ligands of the site has been mutated away (His46), there are not enough ligands left in the metal site to satisfy the need of the Cu(II) for strong ligands. It is concluded that H<sub>2</sub>O or OH<sup>–</sup> completes the coordination sphere of the Cu<sup>2+</sup>, as was found to be the case for the His117Gly mutant (den Blaauwen et al., 1993; Danielsen et al., 1995). The crystallographic data

on the apo-His46Gly mutant are compatible with H<sub>2</sub>O or OH<sup>–</sup> being located in the cavity created by the His to Gly replacement (Hammann et al., 1996).

It is interesting to contrast the His46Gly(H<sub>2</sub>O) findings with those of the His117Gly(H<sub>2</sub>O) variant. In the latter case, the bands around 400 nm (type-2 sites) and 630 nm (type-1 site) are of comparable strength at pH 6 and have been ascribed to two different His117Gly(H<sub>2</sub>O) species (den Blaauwen et al., 1993). In the His46Gly case, the 630 nm absorption (type-1 site) is very weak compared to the 400 nm absorption (type-2 site). Also, the pH behavior of the two mutants is different. The two His117Gly(H<sub>2</sub>O) species are converted into OH<sup>–</sup> species at pH 9 with different optical characteristics and different RR fingerprint spectra (den Blaauwen et al., 1993). For His46Gly azurin, the optical spectrum hardly changes with pH, and the bands simply disappear above pH 8.

**Ligand Binding.** The pronounced changes that occur in the optical spectrum upon addition of ligands to the holo-His46Gly azurin (i.e., the Cu-containing protein) and the observation of isosbestic points (see Figure 5a,b,d,f), indicate that the Cu site in the His46Gly(H<sub>2</sub>O) variant is converted into one or more other species and that the externally added ligand integrates into the first coordination shell of the Cu similar to what has been established for the His117Gly mutant (Danielsen et al., 1995). Sometimes, at high concentrations of ligand, the optical bands begin to bleach (see for instance Figures 5c,e). This is observed especially for some imidazole-like ligands. Apparently the excess of ligand (by more than 2 orders of magnitude) is sufficient to start extracting the Cu from the metal binding site in the protein. This also explains why in these titrations no isosbestic points are observed.

It is remarkable that the equilibrium between ligand-free and ligand-bound holo-His46Gly azurin is always established within a few seconds, despite the cavity being buried in the protein. In combination with the previous observation, it demonstrates that the protein matrix is flexible enough to provide for the passage of a ligand, and that ligand binding is kinetically, but not necessarily thermodynamically, favorable. The slow step in ligand binding as observed with the His117Gly mutant (den Blaauwen & Canters, 1993) is absent in the case of the His46Gly azurin.

In some respects, the results from the ligand addition experiments contrast with previous findings for the His117Gly mutants. With a particular ligand, His46Gly tends to form type-1 and type-2 sites which are in equilibrium. His117Gly, on the other hand, has a preference for the formation of type-1 sites. Furthermore, while the RR frequencies for the type-1 sites in both mutants appear similar for a particular ligand, the main bands for the type-2 site are about 15 cm<sup>–1</sup> higher in the His46Gly than in the His117Gly azurin. This points toward a shorter and stronger Cu–S(Cys) bond in the former case. Third, the metal binding site in the His46Gly protein seems to be less accommodating for external ligands than His117Gly. Ligands like histidine, thiazole, *N*-polyvinylimidazole, and *N*<sup>ω</sup>-acetylhistamine bind to the Cu<sup>2+</sup> in the His117Gly but not in the His46Gly variant. Also, the ligand binding constants appear smaller for His46Gly than for His117Gly.

The temperature effect observed in the optical spectrum of the sample containing excess (0.5 M) chloride requires further comment. In the presence of glycerol, lowering the

temperature from 300 to 77 K causes the optical bands corresponding with the  $\text{Cl}^-$ -bound species to almost disappear and to be replaced by the bands characteristic of the His46Gly( $\text{H}_2\text{O}$ ) species (see Figure 8). This is consistent with the finding that the EPR spectrum of the His46Gly in the presence of 500 mM chloride is almost identical at 77 K with that of the His46Gly( $\text{H}_2\text{O}$ ) sample (Figure 6). The interpretation of this observation is that lowering the temperature promotes dissociation of the  $\text{Cl}^-$ , i.e., it increases  $K_d$ . In the absence of glycerol, the optical bands corresponding to the chloride-bound species also diminish in intensity but not as strongly as in the presence of glycerol. We think the cause for this is that freezing of a concentrated NaCl solution brings about fractionation of the sample, i.e., the separation of a solid pure water phase from a salt- and protein-containing liquid phase (Yang & Brill, 1991). In the absence of glycerol, there is a greater increase in the chloride concentration of the liquid phase during freezing, and this promotes the formation of the chloride-bound species.

**Copper Uptake.** The wt rate constants for copper uptake at pH 6.0 are about a factor of 3 lower than published in 1979 (Marks & Miller, 1979) but are in agreement with the results found in 1963 by Yamanaka et al. The difference can be ascribed to different experimental conditions. In the present study, and in the 1963 study a dilute buffer system of respectively 20 mM Mes and 11 mM phosphate was used while Marks and Miller employed a more concentrated (160 mM) buffer system.

It is remarkable to see that the His46Gly azurin is about 20 times faster in taking up copper than wt. It is known (Marks & Miller, 1979) that the formation of a transitory Cu-protein association complex is the rate-limiting step in the  $\text{Cu}^{2+}$  uptake process. It has been concluded that copper is incorporated into azurin by a mechanism in which His117 scavenges the  $\text{Cu}^{2+}$  from the solution and thus effectively increases the local concentration of the  $\text{Cu}^{2+}$  in the vicinity of the metal binding site [in the literature this has been referred to as the "swinging door" mechanism (Marks & Miller, 1979; Blaszkak et al., 1983; Nar et al., 1992)]. When the  $\text{pK}_a$  of His117 varies, it follows that at a fixed pH the Cu binding capacity of the histidine varies. According to the above mechanism, the rate of Cu uptake would then vary concomitantly. The  $\text{pK}_a$  of His117 in apo-wt and apo-His46Gly azurin is 7.6 (van de Kamp et al., 1990b) and  $6.6 \pm 0.2$  (this study), respectively, and therefore at pH 6.0, the fraction of unprotonated His117 is about 8 times bigger in apo-His46Gly azurin than in apo-wt azurin. This would be sufficient to account for the larger part of the enhanced Cu uptake rate in the case of the His46Gly azurin when compared to wt.

A conspicuous feature of the data in Table 3 is that the Cu uptake by the His46Gly variant is faster than in the case of His117Gly azurin despite the channel created toward the Cu site in the latter case. This is a further indication for the important role of His117 in Cu uptake.

**Redox Properties of His46Gly and His117Gly Azurin.** The possibility of reoxidation of the reduced protein in the presence of  $\text{Cl}^-$  with ammonium peroxydisulfate or by electrochemical means, in combination with the impossibility of reconstitution by adding  $\text{Cu}^{2+}$  after reduction of the protein, shows that the reduced His46Gly and His117Gly azurins retain their  $\text{Cu}^{1+}$ . The suggestion that the copper

site, when reduced, is unstable and undergoes some chemical modification (den Blaauwen & Canters, 1993) is disproven by the observation that reconstitution with  $\text{Cu}^{2+}$  is possible after thiourea treatment.

The reason why it is impossible to reoxidize the reduced His46Gly and His117Gly azurins is not completely clear, but probably has to do with a high midpoint potential of the His46Gly( $\text{H}_2\text{O}$ ) and His117Gly( $\text{H}_2\text{O}$ ) species. There are precedents for an increase in midpoint potential upon loss of histidine coordination in the literature. The copper sites in blue copper proteins like plastocyanin, amicyanin, and pseudoazurin are known in the reduced state to undergo a change in coordination of their Cu under acidic conditions (Guss et al., 1986; Lommen & Canters, 1990; Sykes, 1991; Dennison et al., 1994; Vakoufari et al., 1994). The histidine that protrudes through the surface (the equivalent of His117 in azurin) becomes protonated and dissociates from the Cu. Through this loss of a ligand the Cu becomes three-coordinated, and this strongly stabilizes the Cu(I) over the Cu(II) state. The result is a steep rise in midpoint potential. We think that a similar phenomenon affects the midpoint potentials of the His46Gly( $\text{H}_2\text{O}$ ) and His117Gly( $\text{H}_2\text{O}$ ) species. It is known that compared to Cu(II) the preference of Cu(I) for oxygen-containing ligands is small. Loss of the  $\text{H}_2\text{O}$  ligand upon reduction of the Cu would stabilize again the Cu(I) state and lead to an increase in midpoint potential similar to what is observed for the plastocyanins, amicyanins, and pseudoazurin. The much faster rates by which His46Gly and His117Gly can be reduced (for instance by ascorbic acid), as compared to wt azurin (Parr et al., 1977), are also compatible with a higher midpoint potential of the former two proteins.

It is interesting to note that the His46Gly and His117Gly azurins in the presence of excess chloride remain redox-active. Apparently, the  $\text{Cl}^-$  ion, when present in excess, is still able to bind to the Cu in its Cu(I) state. Nevertheless, the midpoint potential of the His46Gly( $\text{Cl}^-$ ) species is higher than of the wt protein, showing that even in this case the reduced forms of His46Gly( $\text{Cl}^-$ ) and His117Gly( $\text{Cl}^-$ ) are stabilized over the oxidized form when compared to the wt azurin.

## CONCLUSION

The conclusions of the present work can be stated as follows.

Apart from the replacement of His46 by a glycine, the structure of the apo-His46Gly azurin is not appreciably distorted from the wild-type apo structure. In aqueous solution and in the absence of externally added ligands, the coordination sphere of the Cu(II) in the His46Gly azurin is completed by one or two water molecules that substitute for His46, exactly as has been established for the His117Gly( $\text{H}_2\text{O}$ ) species (den Blaauwen et al., 1993). The various absorption bands that are observed around 400 and 630 nm in the optical spectra of His46Gly in the presence and absence of externally added ligands correspond with S(Cys)-Cu charge-transfer transitions as is clearly apparent from the RR spectra. A similar conclusion has been formulated for the His117Gly azurin in previous work (den Blaauwen et al., 1993).

Neither His46 nor His117 is essential for the occurrence of a type-1 Cu site in azurin: in the absence of either

histidine ligand, a type-1 site can be obtained also by adding an appropriately chosen external ligand. A similar conclusion has been reached on the basis of a study of a His46Asp azurin mutant (Germanas et al., 1993) and a His96Asp amicyanin mutant (Dennison et al., 1995).

In the presence of externally added ligands, His46Gly exhibits a tendency to form type-2 sites or an equilibrium mixture of a type-1 and a type-2 species, while His117Gly often forms predominantly type-1 sites.

The covalent attachment of the ligand at position 46 or 117 to the protein backbone is essential for the electron transfer function of the protein. When this link is severed, the protein is not able to rapidly interconvert between the Cu(II) and the Cu(I) forms.

## ACKNOWLEDGMENT

We thank Dr. A. C. F. Gorren from Delft University for assisting us with stopped-flow experiments and the UV/vis measurements at 77 K. Mr. Jingyuan Ai is thanked for the help with the resonance Raman experiments.

## REFERENCES

- Adman, E. T. (1991) *Adv. Protein Chem.* 42, 145–197.
- Adman, E. T., & Jensen, L. H. (1981) *Isr. J. Chem.* 21, 8–12.
- Andrew, C. R., Yeom, H., Valentine, J. S., Karlsson, B. G., Van Pouderoyen, G., Canters, G. W., Loehr, T. M., & Sanders-Loehr, J. (1994) *J. Am. Chem. Soc.* 116, 11489–11498.
- Baker, E. N. (1988) *J. Mol. Biol.* 203, 1071–1095.
- Barrick, D. (1994) *Biochemistry* 33, 6546–6554.
- Blaszak, J. A., McMillin, D. R., Thorton, A. T., & Tennent, D. L. (1983) *J. Biol. Chem.* 258, 9886–9892.
- Canters, G. W. (1987) *FEBS Lett.* 212, 168–172.
- Danielsen, E., Bauer, R., Hemmingsen, L., Bjerrum, M. J., Butz, T., Tröger, W., Canters, G. W., den Blaauwen, T., & van Pouderoyen, G. (1995) *Eur. J. Biochem.* 233, 544–560.
- den Blaauwen, T., & Canters, G. W. (1993) *J. Am. Chem. Soc.* 115, 1121–1129.
- den Blaauwen, T., Van de Kamp, M., & Canters, G. W. (1991) *J. Am. Chem. Soc.* 113, 5050–5052.
- den Blaauwen, T., Hoitink, C. W. G., Canters, G. W., Han, J., Loehr, T. M., & Sanders-Loehr, J. (1993) *Biochemistry* 32, 12455–12464.
- Dennison, C., Kohzuma, T., McFarlane W., Suzuki, S., & Sykes, A. G. (1994) *Inorg. Chem.* 33, 3299–3305.
- Dennison, C., Vijgenboom, E., & Canters, G. W. (1995) *J. Inorg. Biochem.* 59, 667.
- Durley, R., Chen, L., Lim, L. W., Mathews, F. S., & Davidson, V. L. (1993) *Protein Sci.* 2, 739–752.
- Fitzgerald, M. M., Churchill, M. J., McRee, D. E., & Goodin, D. B. (1994) *Biochemistry* 33, 3807–3818.
- Germanas, J. P., Di Bilio, A. J., Gray, H. B., & Richards J. H. (1993) *Biochemistry* 32, 7698–7702.
- Guss, J. M., & Freeman, H. C. (1983) *J. Mol. Biol.* 169, 521–563.
- Guss, J. M., Harrowell, P. R., Murata, M., Norris, V. A., & Freeman, H. C. (1986) *J. Mol. Biol.* 192, 361–387.
- Hammann, C., van Pouderoyen, G., Nar, H., Rueth, F.-X. G., Messerschmidt, A., Huber, R., den Blaauwen, T., & Canters, G. W. (1996) *J. Mol. Biol.* (submitted for publication).
- Han, J., Loehr, T. M., Lu, Y., Valentine, J. S., Averill, B. A., & Sanders-Loehr, J. (1993) *J. Am. Chem. Soc.* 115, 4256–4263.
- Kalverda, A. P., Wymenga, S. S., Lommen, A., Van de Ven, F. J. M., Hilbers, C. W., & Canters, G. W. (1994) *J. Mol. Biol.* 240, 358–371.
- Karlsson, B. G., Nordling, M., Pascher, T., Tsai, L.-C., Sjölin, L., & Lundberg, L. G. (1991) *Protein Eng.* 4, 343–349.
- Kraulis, P. J. (1991) *J. Appl. Crystallogr.* 24, 946–950.
- Kroes, S. J., Hoitink, C. W. G., & Canters, G. W. (1993) *J. Inorg. Biochem.* 51, 176.
- Lommen, A., & Canters, G. W. (1990) *J. Biol. Chem.* 265, 2768–2774.
- Lu, Y., LaCroix, L. B., Lowery, M. D., Solomon, E. I., Bender, C. J., Peisach, J., Roe, J. A., Gralla, E. B., & Valentine, J. S. (1993a) *J. Am. Chem. Soc.* 115, 5907–5918.
- Lu, Y., Casimiro, D. R., Bren, K. L., Richards, J. H., & Gray, H. B. (1993b) *Proc. Natl. Acad. Sci. U.S.A.* 90, 11456–11459.
- Marks, R. H. L., & Miller, R. D. (1979) *Arch. Biochem. Biophys.* 195, 103–111.
- McRee, D. E., Jensen, G. M., Fitzgerald, M. M., Siegel, H. A., & Goodin, D. B. (1994) *Proc. Natl. Acad. Sci. U.S.A.* 91, 12847–12851.
- Mizoguchi, T. J., Di Bilio, A. J., Gray, H. B., & Richards, J. H. (1992) *J. Am. Chem. Soc.* 114, 10076–10078.
- Nar, H., Messerschmidt, A., Huber, R., Van de Kamp, M., & Canters, G. W. (1991a) *J. Mol. Biol.* 218, 427–447.
- Nar, H., Messerschmidt, A., Huber, R., Van de Kamp, M., & Canters, G. W. (1991b) *J. Mol. Biol.* 221, 765–772.
- Nar, H., Messerschmidt, A., Huber, R., Van de Kamp, M., & Canters, G. W. (1992) *FEBS Lett.* 306, 119–124.
- Parr, S. R., Barber, D., & Greenwood, C. (1977) *Biochem. J.* 167, 447–455.
- Pascher, T., Karlsson, B. G., Nordling, M., Malmström, B. G., & Vänggård, T. (1993) *Eur. J. Biochem.* 212, 289–296.
- Peisach, J., & Blumberg, W. E. (1974) *Arch. Biochem. Biophys.* 165, 691–708.
- Petratos, K., Dauter, Z., & Wilson, K. S. (1988) *Acta Crystallogr.* B44, 628–636.
- Romero, A., Hoitink, C. W. G., Nar, H., Huber, R., Messerschmidt, A., & Canters, G. W. (1993) *J. Mol. Biol.* 229, 1007–1021.
- Romero, A., Nar, H., Huber, R., Messerschmidt, A., Kalverda, A. P., Canters, G. W., Durley, R., & Mathews, F. S. (1994) *J. Mol. Biol.* 236, 1196–1211.
- Sambrook, J., Fritsch, E. F., & Maniatis, T. (1989) *Molecular cloning*, Cold Spring Harbor Laboratory, Cold Spring Harbor, NY.
- Sykes, A. G. (1991) *Adv. Inorg. Chem.* 36, 377–408.
- Vakoufari, E., Wilson, K. S., & Petratos, K. (1994) *FEBS Lett.* 347, 203–206.
- van de Kamp, M., Silvestrini, M. C., Brunori, M., Van Beeumen, J., Hali, F. C., & Canters, G. W. (1990a) *Eur. J. Biochem.* 194, 109–118.
- van de Kamp, M., Hali, F. C., Rosato, N., Finazzi-Agro, A., & Canters, G. W. (1990b) *Biochim. Biophys. Acta* 1019, 283–292.
- van de Kamp, M., Canters, G. W., Wijmenga, S. S., Lommen, A., Hilbers, C. W., Nar, H., Messerschmidt, A., & Huber, R. (1992) *Biochemistry* 31, 10194–10207.
- Vänggård, T. (1972) in *Biological Application of Electron Spin Resonance* (Swartz, H. M., Bolton, J. R., & Borg, D. C., Eds.) pp 411–417, Wiley-Interscience, New York.
- van Pouderoyen, G., Mazumdar, S., Hunt, N. I., Hill, H. A. O., & Canters, G. W. (1994) *Eur. J. Biochem.* 222, 583–588.
- Wilks, A., Sun, J., Loehr, T. M., & Ortiz de Montellano, P. R. (1995) *J. Am. Chem. Soc.* 117, 2925–2926.
- Yamanaka, T., Kijimoto, S., & Okunuki, K. (1963) *J. Biochem.* 53, 256–259.
- Yang, A.-S., & Brill, A. S. (1991) *Biophys. J. Biophys. Soc.* 59, 1050–1063.

BI951604W